Signatures of an annular Fermi sea

Insun Jo, Yang Liu, L. N. Pfeiffer, K. W. West, K. W. Baldwin, and M. Shayegan*
Department of Electrical Engineering, Princeton University, Princeton, New Jersey 08544, USA

R. Winkler
Department of Physics, Northern Illinois University, Dekalb, Illinois 60115, USA

(Received 30 June 2016; revised manuscript received 1 November 2016; published 3 January 2017)

The concept of a Fermi surface, the constant-energy surface containing all the occupied electron states in momentum, or wave-vector (k), space plays a key role in determining electronic properties of conductors. In two-dimensional (2D) carrier systems, the Fermi surface becomes a contour which, in the simplest case, encircles the occupied states. In this case, the area enclosed by the contour, which we refer to as the Fermi sea (FS), is a simple disk. Here we report the observation of an FS with a new topology, namely, an FS in the shape of an annulus. Such an FS is expected in a variety of 2D systems where the energy band dispersion supports a ring of extrema at finite k, but its experimental observation has been elusive. Our study provides (1) theoretical evidence for the presence of an annular FS in 2D hole systems confined to wide GaAs quantum wells and (2) experimental signatures of the onset of its occupation as an abrupt rise in the sample resistance, accompanied by a sudden appearance of Shubnikov–de Haas oscillations at an unexpectedly high frequency whose value does not simply correspond to the (negligible) density of holes contained within the annular FS.

DOI: 10.1103/PhysRevB.95.035103

Many properties of conductors are influenced by the shape, connectivity, and topology of their Fermi sea (FS) [1,2]. Figure 1 highlights examples of FSs in two-dimensional (2D) systems. The simplest FS, a connected disk, is shown in Fig. 1(a). In 2D systems with multiple conduction band valleys, e.g., 2D electrons confined to Si or AlAs quantum wells (QWs) [3–5], or 2D electrons in a wide GaAs QW subject to very large parallel fields [6], the FS consists of a number of separate sections, each containing a fraction of the electrons in the system [Fig. 1(b)]. Figure 1(c) shows yet another possible FS topology, namely, an *annulus*, which is the subject of our study. The existence of such an FS, emerging from an inverted energy band with a ring of extrema at finite k, has been discussed for many systems; e.g., those with a strong spin-orbit interaction (SOI) [7–14], biased bilayer graphene [15–19], and monolayer Ga chalcogenides [20,21]. Moreover, since the electron states near the band extremum become highly degenerate, resulting in a van Hove singularity in the density of states, an annular FS has been predicted to host exotic interaction-induced phenomena and phases such as ferromagnetism [19–21], anisotropic Wigner crystal and nematic phases [22–26], and a persistent current state [18].

Although the possibility of an annular FS has long been recognized theoretically, its experimental detection has been elusive. For the cases in Figs. 1(a) and 1(b), the FS can readily be probed via magnetotransport measurements as the frequencies of the Shubnikov–de Haas (SdH) oscillations, multiplied by e/h, directly give the FS area or, equivalently, the areal density of the 2D system [4–6,27–29]; e is the electron charge and h is the Planck constant. For the annular FS case in Fig. 1(c), however, no data have been reported. Nor is it known how the SdH oscillations should behave or how their frequencies are related to the area of the annular FS. Here we report energy band calculations and experimental data,

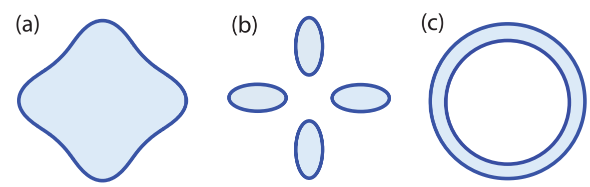

FIG. 1. Examples of Fermi seas in 2D systems: (a) simple disk, (b) multifold ellipses, (c) annulus.

demonstrating the realization of an annular FS and its unusual SdH oscillations in 2D hole systems (2DHSs) confined in wide GaAs QWs.

Figure 2 captures the key points of our study. Figures 2(a) and 2(b) show the calculated energy band dispersions for a 2DHS at a density of $p = 1.20 \times 10^{11}$ cm^{-2} confined in a 38-nm-wide GaAs QW. The self-consistent calculations are based on the 8×8 Kane Hamiltonian [14]. The charge distribution is bilayerlike (Fig. 2(d)) because the Coulomb repulsion pushes the carriers (holes) towards the confinement walls [30–32]. As shown in Figs. 2(a) and 2(b), the energy band dispersion is very unusual, showing an *inverted* structure for the excited subband with a "ring of maxima" at finite values of k. So far, such dispersions were studied mostly within systems with the Rashba SOI [7–12,14]. However, in our symmetric 2DHS (without the Rashba SOI), the inverted band structure stems from the combined effect of a strong level repulsion between the second heavy-hole and the first light-hole subbands at $k > 0$ [33] as well as the Dresselhaus SOI [34]. Because such a band structure exists near the bottom of the excited subband, it is experimentally accessible at a moderate density of carriers in wide QWs. Additionally, high-density carriers in the ground subband screen the ionized impurity scattering so that carriers in the excited subband can have a relatively high mobility even at a low density. When holes start to occupy the excited subband, its FS adopts an annular shape [Fig. 2(c)]. Unlike the FS of the ground subband, the annular FS has a void for small

*Corresponding author: shayegan@princeton.edu

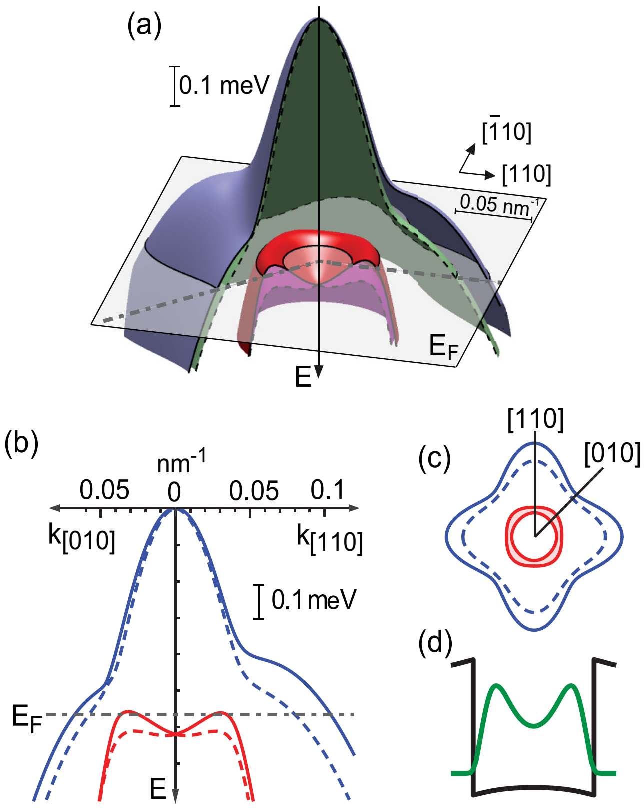

FIG. 2. (a, b) Calculated subband energy dispersions for GaAs 2D holes in a 38-nm-wide GaAs QW at density $p = 1.2 \times 10^{11}$ cm^{-2}. Upper (lower) dispersions are for the ground (excited) subbands, each consisting of two spin-split branches at finite k, shown by solid and dashed lines. The horizontally cut plane in (a) and the dash-dotted line in (b) represent the Fermi energy. In (b) the energy dispersions are shown along two directions. (c) Fermi contours for the ground (blue) and excited (red) subbands. FSs for the ground subband are not colored, for clarity; the FS for the excited subband is the red annulus. (d) Hole charge distribution (green line) and potential (black line).

k. In our experiments we probe the energy band dispersions via monitoring the sample resistance and also measuring SdH oscillations as a function of the density. As the holes start to occupy the excited subband, we observe an abrupt rise in the sample resistance and the sudden appearance of an extra peak at a relatively high frequency in the Fourier transform (FT) spectra. We associate this peak with the annular FS and discuss the details of its evolution with increasing hole density.

We used 40- and 35-nm-wide, symmetric, GaAs QWs grown by molecular beam epitaxy along the [001] crystal direction. Here we focus on data for the 40-nm-wide QW; we observe qualitatively similar data for the narrower QW, as presented in Appendix D. The QWs are symmetrically modulation doped with two C δ-doped layers. We used two 40-nm-wide QW samples with different $Al_{0.3}Ga_{0.7}As$ spacer-layer thicknesses (160 and 90 nm), different as-grown hole densities ($p = 1.3$ and 2.0, in units of 10^{11} cm^{-2}, which we use throughout this paper), and different mobilities (32 and 76 m^2/Vs). The data for $p \leqslant 1.43$ are taken from the lower density sample, and the higher density data from the other sample. In each sample, front- and back-gate electrodes allow us to change independently the 2D hole density and the asymmetry of the charge distribution in the QW. In this study, we focus on symmetric charge distributions; we judge the symmetry via a careful examination of the SdH oscillations in the low-density regime where only the ground subband is occupied [35], as well as the strengths of fractional quantum Hall states, e.g., at $\nu = 1/2$ [32]. The low-field magnetoresistance oscillations are measured in a dilution refrigerator at a base temperature of ~50 mK.

Figure 3 shows the evolutions of low-field magnetoresistance data [Fig. 3(a)], their corresponding FT spectra [Fig. 3(b)], the calculated energy dispersions [Fig. 3(c)], and the associated Fermi contours [Fig. 3(d)] [36]. For clarity, the traces in Fig. 3(a) and their FTs in Fig. 3(b) are shifted vertically. The intensities of the FTs are normalized so that the heights of the strongest FT peaks in different spectra are comparable. For all traces the total density is determined from the position of the high-frequency peak that is marked by an open circle following Onsager [28], i.e., by multiplying the frequency by e/h. This density agrees, to within 4%, with the magnetic-field positions of the integer and fractional quantum Hall states observed at high fields. At low densities ($p < 1.2$) the FT spectra are simple. Besides a peak corresponding to the total density, we also observe a second peak, marked by a filled blue circle, at half the value of the total density peak. We associate this peak with SdH oscillations of the ground-subband holes at very low magnetic fields where the Zeeman energy is low and the spin splitting of the Landau levels is not yet resolved.

As the density is raised to $p = 1.20$, an FT peak suddenly appears at $\simeq 1.5$ T in Fig. 3(b). This peak, which is shown by the red arrow and circle on the $p = 1.20$ trace, signals the onset of the excited-subband occupation [37]. As we discuss later, there is also a rather sharp rise in the sample resistance at $p = 1.20$ (Fig. 4), consistent with our conjecture. This new FT peak has two unusual characteristics. First, its emergence is very abrupt. It is essentially absent at the slightly lower density of $p = 1.16$, and its strength grows very quickly, to become the dominant peak in the whole FT spectrum at the slightly higher density of $p = 1.25$. Second, its frequency, multiplied by the usual factor (e/h or $2e/h$), clearly does *not* give the correct density of holes in the excited subband, which we expect to be extremely low, essentially zero at the onset of excited-subband occupation. Consistent with this expectation, the peak near 2.5 T (shown by the blue circle), which we associate with the ground subband, indeed accounts for essentially *all* the QW's holes: 2.5 T multiplied by $2e/h$ gives $p = 1.20$, leaving very few holes for the excited subband. Hence we conclude that the frequency of the $f \simeq 1.5$ T peak is not simply related to the excited-subband density. This is in sharp contrast to the GaAs 2D *electron* systems where, after the onset of the excited-subband occupations, an FT peak appears at a low frequency which correctly gives the electron density of the excited subband, and this peak's frequency increases slowly and continuously as more electrons occupy the excited subband [27,38–42].

We associate the $f \simeq 1.5$ T peak appearing at the onset of the excited-subband occupation with the formation of an annular FS in our 2DHS. But how should an annular FS be manifested in SdH oscillations? Given that the frequency of this peak does not correspond to the area of the annulus, is

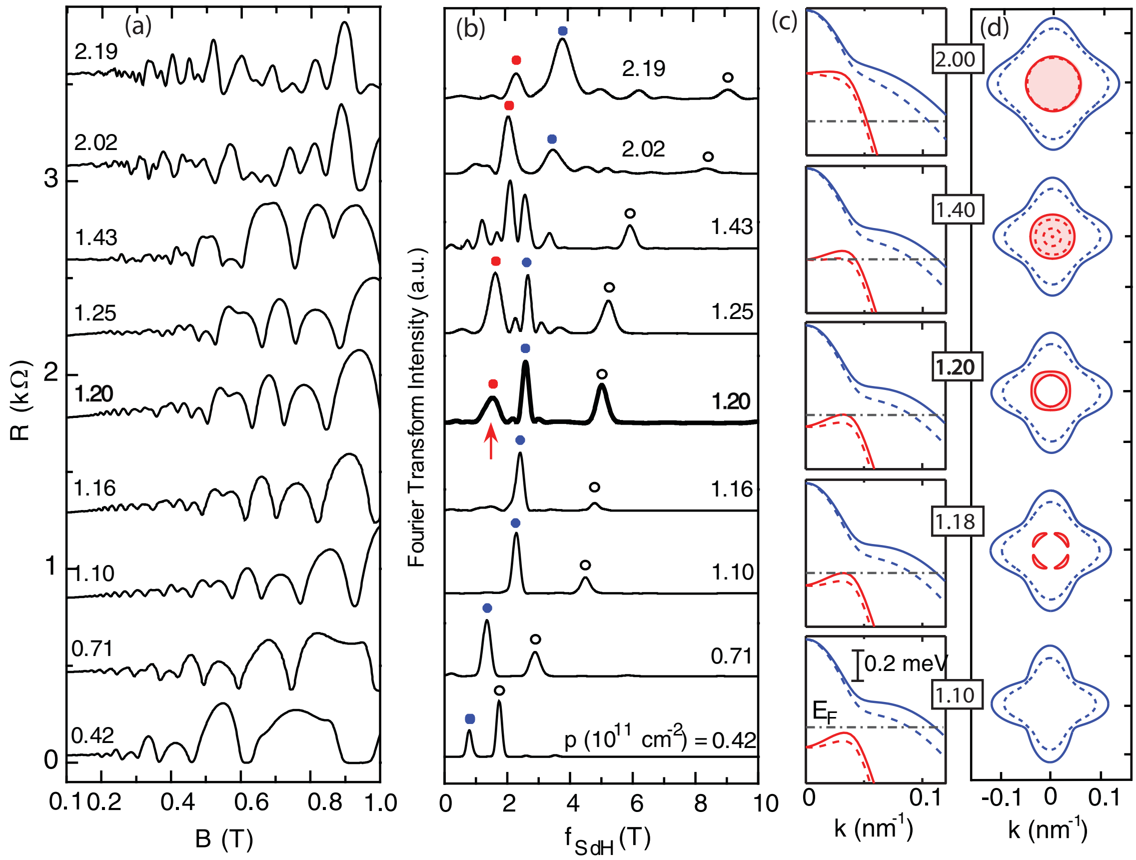

FIG. 3. (a) Low-field magnetoresistance traces at different densities. (b) Fourier transform spectra of the SdH oscillations at each density. Open circles indicate total density peaks. Blue and red circles mark the peaks associated with the ground and excited subbands; respectively. (c) Calculated energy dispersions and (d) Fermi sea, at densities $p = 1.10, 1.18, 1.20, 1.40$, and 2.00×10^{11} cm^{-2}, from bottom to top. Dash-dotted gray lines in (c) represent the Fermi energy. In (c) and (d), blue and red lines correspond to ground and excited subbands, respectively; solid and dashed lines represent spin-split states.

there an alternative relation? Following Onsager [28], one may conjecture that it could lead to oscillations whose frequencies are given by the areas enclosed by the outer and inner circles (or more generally, the "contours") of the annulus, namely, by the areas πk_o^2 and πk_i^2, where k_o and k_i are the radii of the outer and inner circles [see the Fermi contour for $p = 1.20$ in Fig. 3(d)]. Near the onset of the excited-subband occupation, the outer and inner contours of the annulus are very close to each other, implying that the FT should show two closely spaced peaks or one broad peak (if these two peaks cannot be resolved), qualitatively consistent with our data. Quantitatively, based on the energy band calculations for $p = 1.20$, we would expect FT peaks at $f = 0.43$ T and $f = 0.27$ T for the outer and inner rings, respectively. These values are smaller than the frequency ($f \simeq 1.5$ T) of the broad peak we observe in the FT. This discrepancy might imply that the semiclassical description is not entirely correct or that the band calculations without considering the exchange energy are not quantitatively accurate near the bottom of the excited subband. Additionally, quantum mechanical effects for a k-space trajectory in the annulus can cause corrections to the semiclassical description of the SdH oscillations [43–45].

The evolution of the FT spectra for $p > 1.20$ is also suggestive. For $p = 1.43$, e.g., the spectrum becomes quite complex, showing multiple peaks near 2 T. This is qualitatively consistent with the results of the energy band calculations: Near the onset of the excited-subband occupation, E_F can have four crossings with the excited-subband dispersion (two for each spin-subband dispersion), resulting in two complex annular FSs [see Figs. 3(c) and 3(d) for $p = 1.40$]. As we further increase the density, the FT spectra become simpler, showing two dominant peaks at the highest densities [see FTs for $p = 2.02$ and 2.19 in Fig. 3(b)]. Such an evolution qualitatively agrees with our expectation based on the calculated bands, which indicate two "disklike" FSs (i.e., without voids at $k = 0$), one for each subband. Also consistent with calculations, these peaks move to higher frequencies when the densities of subbands increase with increasing total density. If we assign these peaks to the areas of the FSs for the ground and excited subbands, multiply their frequencies by $2e/h$, and sum the two densities, we find a total density which is ~30% higher than the total density expected from the open circles. If we assume that the excited-subband Landau levels are spin-resolved and multiply the lower frequency (red) peak by e/h (instead of $2e/h$), then we obtain a total density which agrees to better than ~8% with the total density deduced from the open circles.

We also measured the zero-field resistance of the 2DHS as a function of the total density in the QW. The data, shown

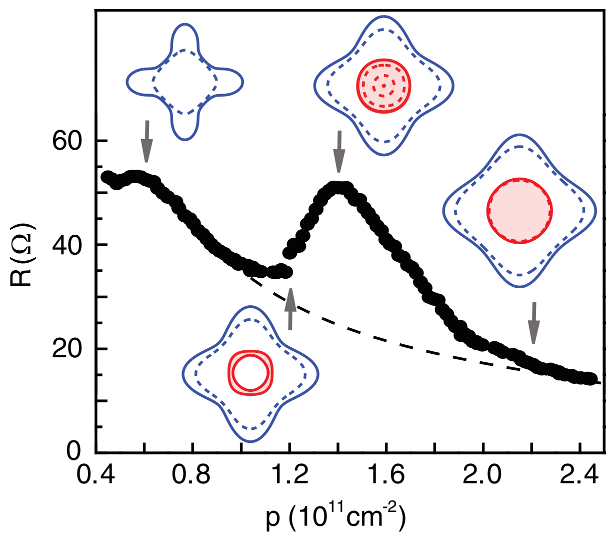

FIG. 4. Zero-field resistance as a function of density. Fermi seas are shown for four densities, indicated by arrows. The dashed line is a guide for the eye.

in Fig. 4, provide corroborating, albeit indirect, evidence for our conclusions. At low densities ($p < 1.2$), where only the ground subband is occupied, the resistance decreases with increasing density, consistent with an increase in conductivity because of the higher hole density and higher mobility. At $p \simeq 1.2$, the resistance shows an abrupt and significant increase. A qualitatively similar rise is also seen at the onset of the occupation of the excited subband in GaAs 2D electrons [38–40] and can be attributed to the enhanced intersubband scattering. In Fig. 4, the resistance remains high in the density range $1.2 < p < 1.8$, where in our experiments we observe multiple, anomalous peaks in the FT spectra [see, e.g., data for $p = 1.25$ and 1.43 in Fig. 3(b)]. For $p \geqslant 1.8$, the resistance returns to low values as the SdH oscillaions and their FTs become simple again, signaling that E_F has gone past the inverted band dispersion.

Before closing, we make two remarks. First, right at the onset of the excited-subband occupation and in an extremely narrow density range near $p = 1.18$, the calculated FS of the excited subband consists of four "arcs" [see Fig. 3(d)]. We do not seem to observe the signature of such an FS in SdH measurements, likely because of the extremely low density of holes in the arcs and, also, because of the very narrow density range where the arcs prevail. Second, techniques such as angle-resolved photoemission spectroscopy (ARPES) could in principle be used to probe the annular FS we study. However, the relevant energy scale of the inverted energy band we are probing is only ~ 0.1 meV [see Fig. 2(b)], well below the energy resolution of state-of-the-art ARPES measurements ($\sim$ 1 meV) [46]. Our SdH data therefore provide a unique probe of such annular FSs.

In conclusion, our study of low-field SdH oscillations for 2D holes confined in a wide QW reveals signatures of an annular FS that originates from the inverted dispersion of the excited subband. When the excited subband begins to be populated, in the FT spectrum we observe the sudden emergence of an anomalous peak whose frequency is not associated with the density of holes in the excited subband through the usual Onsager relation. We add that near the onset of this population, the holes in the excited subband occupy only one spin branch of the dispersion. This is qualitatively different from the usual case (e.g., the ground subband) where, in the absence of the linear-k SOI, the holes occupy both spin subbands even at the onset of the occupation. Our results should stimulate future experimental and theoretical studies of the unusual dispersion and annular FS.

We appreciate stimulating discussions with S. Chesi, D. Culcer, R. J. Joynt, J. Jung, L. Smrcka, K. Vyborny, and U. Zülicke. We acknowledge support from the DOE BES (Grant No. DE-FG02-00-ER45841) grant for measurements and the NSF (Grants No. DMR 1305691, No. DMR 1310199, and No. MRSEC DMR 1420541), the Gordon and Betty Moore Foundation (Grant No. GBMF4420), and the Keck Foundation for sample fabrication and characterization. We also acknowledge support from the NSF for low-temperature equipment (Grant No. DMR MRI 1126061).

APPENDIX A: CONTRAST BETWEEN FERMI SEAS FOR 2D ELECTRONS AND HOLES

Two-subband systems containing high-mobility 2D electrons confined in a GaAs QW have been studied previously [29,38–42,47]. Since the energy dispersions of both ground and excited subbands are parabolic, the FSs are simple, circular disks over a wide density range. In Fig. 5, we schematically show the energy dispersions for electrons [Fig. 5(a)] and holes [Fig. 5(b)] and the shapes of their FSs. In wide QWs, where the energy separation between the ground and the excited subbands is small, the Fermi energy (E_F), denoted by dash-dotted gray lines in Fig. 5, can be tuned to reach the excited subband by increasing the density of carriers. In Fig. 5, the E_F for three representative regimes is shown: (i) E_F is located in the ground subband, (ii) E_F is just past the edge of the excited subband, and (iii) E_F is well beyond the onset of the excited subband occupation. For each regime,

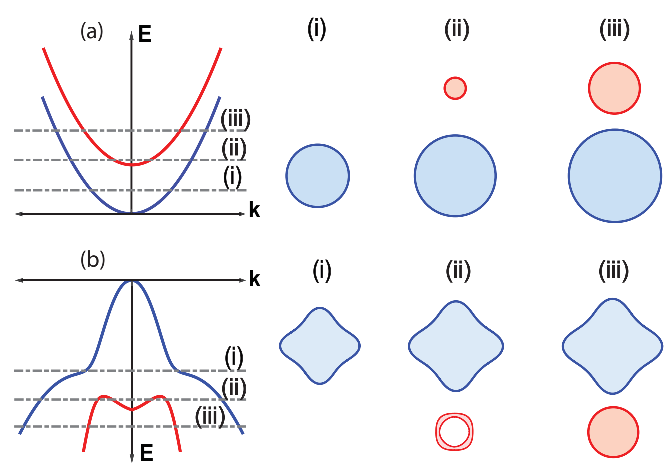

FIG. 5. Schematic energy dispersions for (a) electrons and (b) holes confined to wide GaAs QWs. The blue (red) curve represents the ground (excited) subband. Dash-dotted (gray) lines show different positions of the Fermi energy.

the shapes of FSs for the ground (blue) and excited (red) subbands are shown in the right panels. The focus of our study is in regime (ii), where the annular FS develops for the case of holes [Fig. 5(b)]. In contrast, for electrons, the shape of the FS is always circular for both the ground and the excited subbands.

APPENDIX B: TWO-SUBBAND ELECTRON SYSTEM WITH CIRCULAR FERMI SEAS

The SdH oscillations data and their Fourier transform spectra for 2D *electrons* confined in a 45-nm-wide GaAs QW are shown in Figs. 6(b) and 6(c), respectively [40], together with a summary plot in Fig. 6(a). A front-gate voltage, V_g, is applied to change the density, or E_F. The traces for $V_g \leqslant -0.2$ V show simple FT spectra, each with a single peak, marked by a filled triangle. This peak corresponds to the spin-unresolved carriers [i.e. $n = 2(e/h)f_{\rm SdH}$]. (Because of the small g factor for GaAs 2D electrons, Zeeman spin-splitting is not present in the low-field range used for the FT analysis, leading to the absence of a spin-resolved peak in the FT spectra.) When $V_g \geqslant -0.1$ V, E_F moves past the bottom of the excited subband [case (ii) in Fig. 5(a)]. As a result, an FT peak corresponding to the excited subband appears at $\simeq$0.8 T, as shown by the open triangle at $V_g = -0.1$ V in Fig. 6(c). As the density increases further, both peak positions move toward higher frequencies. The two FT peaks represent the densities of electrons in the ground and excited subbands, and the sum of the two densities agrees very well with the total density over the entire density range [40,41]. The lines drawn through the data points in Fig. 6(a) are the results of self-consistent, local-density-approximation calculations. They agree quite well with the measured data.

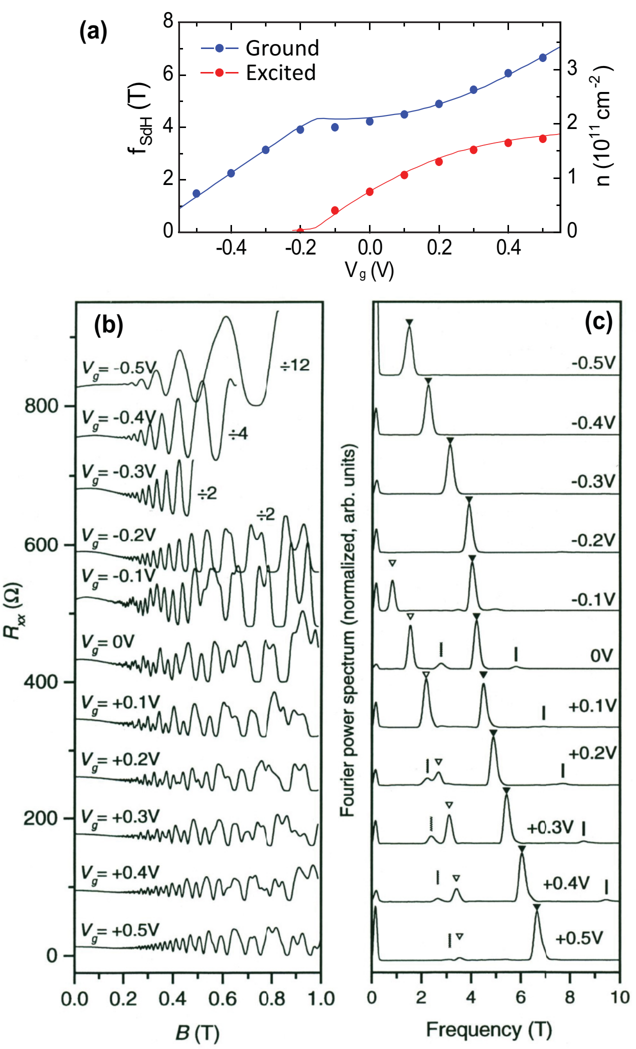

FIG. 6. (a) Summary of FT frequencies measured for 2D electrons confined in a 45-nm-wide GaAs QW at different front-gate voltages (V_g). Ground and excited subband densities are obtained by multiplying $2e/h$ and $f_{\rm SdH}$. Red and blue lines represent the results of self-consistent, local-density-approximation calculations. (b) Low-field SdH oscillations measured at different V_g values. Increasing V_g increases the density and therefore E_F. (c) FT spectra of the corresponding traces in (b). Filled (open) triangles represent the spin-unresolved peak of the ground (excited) subband. Vertical lines indicate the sum and/or difference of the two prominent peaks. Data are taken from Ref. [40].

Other small peaks, shown by vertical lines, are also observed at the sum and difference of the two major peak positions. The frequency corresponding to the sum of two major peak frequencies is expected when the Landau levels are sharp [48]. The frequency corresponding to the difference between two major peak frequencies can be explained by the intersubband scattering [49].

As we emphasize in the text, there are distinct characteristics observed in the FT spectra of circular vs annular FSs for the excited subband of 2D electrons and holes. Two-dimensional electrons, forming only *circular* FSs as shown in Fig. 5(a), exhibit a smooth transition of the FT frequencies [see Figs. 6(a) and 6(c)]. Also, the total density always agrees with the sum of the two frequencies multiplied by $2e/h$, following Onsager's relation [28]. In contrast, in the case of the annular FS, an anomalous FT peak appears abruptly at a finite frequency. Moreover, the sum of the FT frequencies is larger than the total density peak position when the annular FS develops [see Figs. 3(b) and 3(c)].

APPENDIX C: SHUBNIKOV–DE HAAS OSCILLATIONS OF AN ANNULAR FERMI SEA VIA INVERSE FOURIER TRANSFORM

In Fig. 3(b), we observe a finite-frequency peak at $f \simeq$ 1.5 T in the FT of SdH oscillations for our 2D hole system at $p = 1.20$ (p is the total 2D hole density in units of 10^{11} cm^{-2}). We associate this peak with the onset of excited subband occupation and the resulting annular FS. Here we demonstrate that the SdH oscillations corresponding to the annular FS exhibit clear low-field oscillations, which are nearly periodic in $1/B$. In order to extract the SdH oscillations induced by the annular FS, we perform *inverse* FTs for individual peaks as shown in Fig. 7.

In Fig. 7, we show two examples of inverse FT analyses performed at $p = 1.10$ and 1.20. Figures 7(a)–7(c) are for $p = 1.10$, and Figs. 7(d)–7(f) for $p = 1.20$.

When only the ground subband is occupied ($p = 1.10$), we observe two peaks in the FT spectrum [Fig. 7(a)]; the lower (higher) frequency peak corresponds to the spin-unresolved (spin-resolved) SdH oscillations. The observation of the spin-

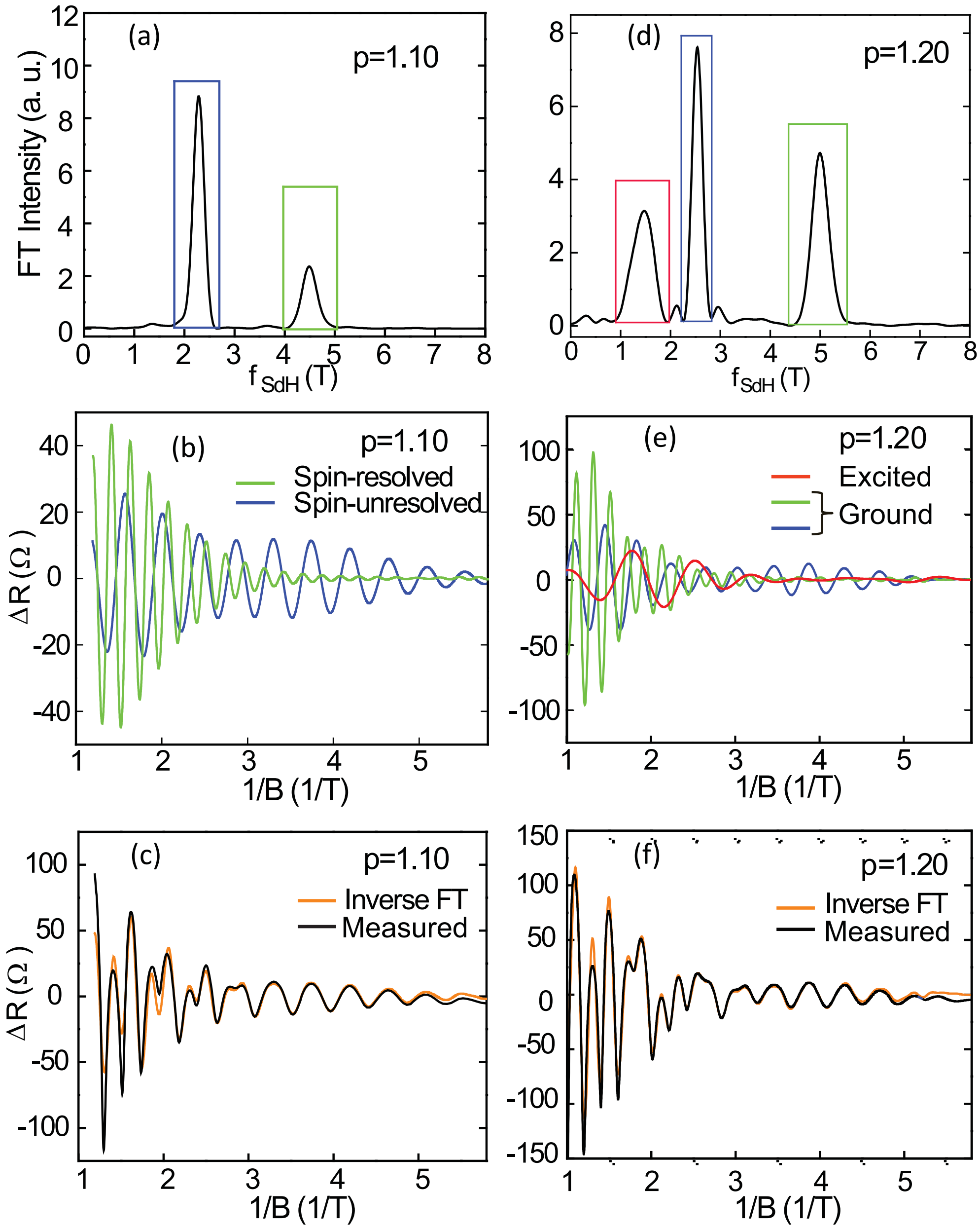

FIG. 7. (a) FT spectrum of SdH oscillations at $p = 1.10$ for the 40-nm-wide GaAs QW presented in the text. Color-coded boxes indicate the square window function applied before implementing inverse FT. (b) Results of inverse FT for each peak. Spin-resolved (spin-unresolved) SdH oscillations are constructed by using the total (half-density) peak in (a). (c) The sum of the two curves in (b) gives the full SdH oscillations (orange curve). Measured data (black line) after a background subtraction are shown for comparison. (d) FT spectrum of SdH oscillations at $p = 1.20$. The additional peak associated with the annular FS is observed at $f \simeq 1.5$ T. (e) SdH oscillations for the ground and excited subbands are obtained after performing inverse FT of the peaks marked with boxes in (d): blue and green for the spin-unresolved and spin-resolved oscillations of the ground subband and red for the excited subband. (f) The sum of the three curves in (e) is shown as an orange curve and is compared with the measured data (black curve).

resolved peak stems from the Zeeman spin-splitting in the field range where the SdH oscillations are analyzed. We apply a square window function to each peak and perform inverse FT separately. The results are shown in Fig. 7(b), where the green (blue) curve represents spin-resolved (spin-unresolved) SdH oscillations. The oscillations are periodic in $1/B$ for each curve, and the period of the green curve is twice the period of the blue curve. As shown in Fig. 7(c), when these two primary oscillations are added to produce the resulting SdH oscillations (orange curve), it agrees very well with the measured data (black curve).

For $p = 1.20$, near the onset of the excited subband occupation, we observe three major peaks in the FT spectrum [Fig. 7(d)]. Two peaks [shown by the blue and green windows in Fig. 7(d)] are associated with the ground subband, while the peak marked by the red window is from the excited subband. In Fig. 7(e), the inverse FTs of these peaks are shown in their respective colors. The blue and green curves in

Fig. 7(e) are qualitatively similar to those in Fig. 7(b) except for the slightly smaller periods of the oscillations, consistent with the 10% higher density of the ground subband (1.20 compared to 1.10). In Fig. 7(e), we also show (red curve) the inverse FT of the anomalous peak (red window) in Fig. 7(d), which we associate with the excited subband. We find that the red curve in Fig. 7(e) is indeed reasonably periodic in $1/B$, except that its period varies between 1.4 and 1.8 T in the range $1 < 1/B < 5\ \mathrm{T}^{-1}$. This variation is consistent with the excited-subband peak in Fig. 7(d) being broad compared to the other two (ground-subband) peaks in the same FT spectrum. We note that the extra width of this peak is not due to its low frequency (∼1.5 T); as shown in Fig. 3, the peak marked by the blue circle for $p = 0.71$ has a similar frequency but is much narrower.

It is not obvious what causes the extra broadening of the excited subband peak. As we state in the text, it might be that there are two peaks (corresponding to areas enclosed by the outer and inner contours of the annular FS) and that we cannot resolve the two peaks. Another possibility is the "magnetic blurring" discussed in Ref. [44]. When the area of the annular FS is smaller than the square of the inverse magnetic length, the momentum-space area can be blurred [44]. If we compare the momentum-space area of the annular FS at $p = 1.20$ with $(1/l_B)^2$, such a blurring could happen for $B > 1.0$ T. Because the field range we use for FT analysis is less than 1.0 T, this blurring should not be relevant for our sample. On the other hand, if we use the criterion $(k_o - k_i) > 1/l_B$, then we conclude that, based on the energy band calculations for $p = 1.20$, which predict $k_o - k_i = 0.0086\ \mathrm{nm}^{-1}$, there should be magnetic blurring for $B > 0.04$ T, i.e., that there should be corrections in the entire range of our measurements. Similarly, for $p = 1.25$ where $(k_o - k_i) = 0.017\ \mathrm{nm}^{-1}$, the magnetic blurring should affect the SdH oscillations for $B > 0.19$ T.

We conclude that the inverse FT technique we present here effectively extracts the SdH oscillations originating from the annular FS of the excited subband.

APPENDIX D: RESULTS FOR 2D HOLES CONFINED TO A 35-NM-WIDE GaAs QW

We also made measurements on a 35-nm-wide QW and observed similar signatures of an annular FS as summarized in Fig. 8. The QW structure is similar to that of the 40-nm QW, and the density of the as-grown sample is $p = 1.63$. Using the front and back gates, we tune the density while keeping the charge distribution of the QW symmetric. We show FT spectra of the SdH oscillations at different densities in Fig. 8(a). Figures 8(b) and 8(c) show the energy dispersions and the Fermi contours for three representative densities, $p = 1.40$, 1.60, and 2.00. Numerical calculations for this narrower QW also indicate the presence of an annular FS near the onset of the excited subband occupation.

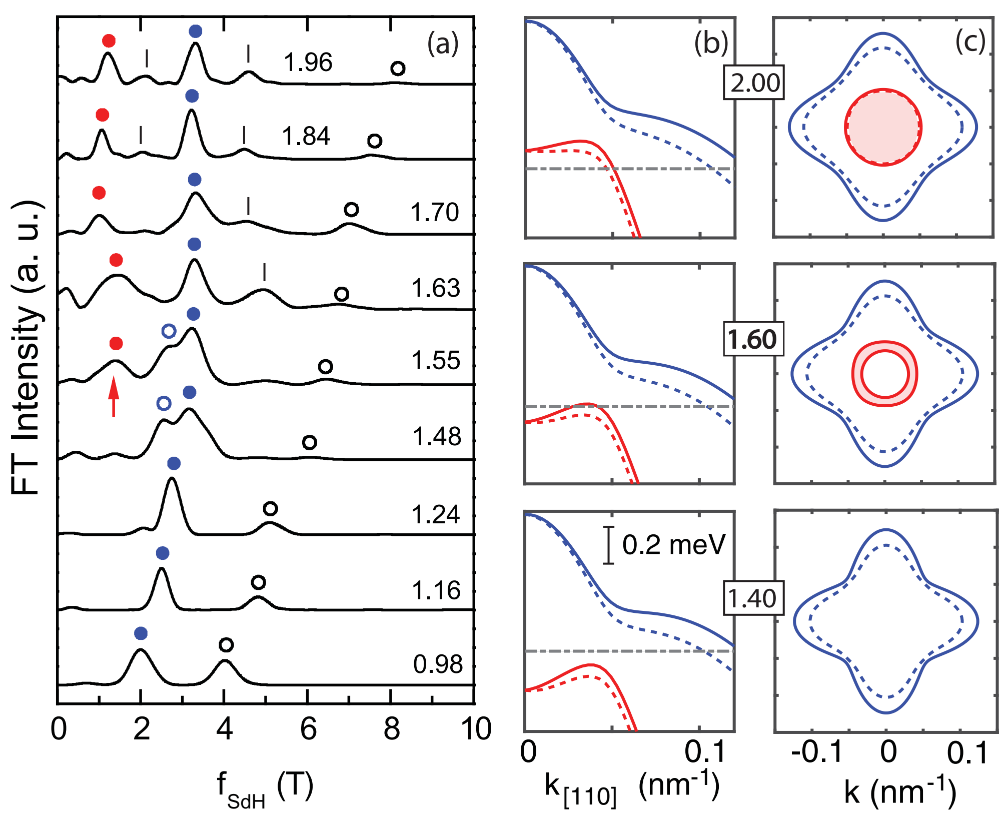

FIG. 8. (a) Fourier transform spectra of the SdH oscillations at different densities measured for 2D holes confined in a 35-nm-wide GaAs QW. Blue (red) circles represent the peaks associated with the ground (excited) subband, while open circles indicate the total density peaks. Vertical lines indicate the sum and/or difference of the two prominent peaks. (b) Calculated energy dispersions and (c) Fermi contours at densities $p = 1.40$, 1.60, and 2.00. Blue (red) lines represent ground (excited) subbands. Calculations were performed for a slightly narrower QW, of width 34 nm, to match the measured onset of the excited subband occupation.

The evolution of FT spectra of the SdH oscillations is shown in Fig. 8(a). At low densities, $p \leqslant 1.24$, the FT spectra show two peaks, representing the spin-unresolved (blue circles) and spin-resolved (open black circles) SdH oscillations for the ground subband, respectively. When $p = 1.48$, we observe a splitting of the ground-subband peak, suggesting that the ground-subband SdH oscillations become spin-resolved. When the density is increased to $p = 1.55$, an additional broad peak appears at $f \simeq 1.4$ T, indicated by the red arrow, which we associate with the annular FS in the excited subband. This peak persists and becomes stronger at $p = 1.63$. This anomalous peak exhibits two distinct features, similar to what we observe for the 40-nm-wide QW. (i) The peak appears abruptly at a finite frequency. (ii) The frequency of the peak does *not* correspond to the excited-subband density (if we use the Onsager relation) when the annular FS is formed.

When the density increases further, the anomalous peak shifts to a slightly smaller value, shown by red circles. This peak grows slowly and continuously with increasing density and, eventually, represents the density of the excited subband when its FS becomes a simple disk ($p \geqslant 1.84$).

We also find some differences between the two samples with different well widths. Compared to the 40-nm-wide QW, the onset of the excited-subband occupation occurs at a higher density, $p = 1.55$, for the 35-nm-wide QW. This is expected because the energy separation between the ground and the excited subband is larger for a narrower QW. In addition, the finite frequency peak for the 35-nm-wide QW is seen at $f \simeq 1.4$ T, which is slightly smaller than the $f \simeq 1.5$ T we observe for the 40-nm-wide QW. The energy band calculations shown in Fig. 8(b) are also consistent with our observations. Compared to the 40-nm-wide QW, the outer radius of the annulus at the onset of the excited subband occupation is about 8% smaller for the 35-nm-wide QW.

In the FT spectra for $p = 1.48$ and 1.55 in Fig. 8(a), we also observe a splitting of the ground-subband peak; we show this splitting by the filled and open blue circles in these two spectra. This splitting is indeed expected from our energy band calculations [see solid and dashed Fermi contours in Fig. 8(c)]. However, it is unclear why we do not observe a similar splitting for the 40-nm-wide QW sample [Fig. 3(b)]. Also, in Fig. 8(a), there are some extra peaks for $p \geqslant 1.63$, which we show by vertical lines. These can be associated with sums and/or differences of the main peaks (shown by red and blue circles), qualitatively similar to the 2D electron data [see Fig. 6(c)].

Despite the differences in the data for the 40- versus the 35-nm-wide QW samples, the clear common feature is the sudden appearance of a broad FT peak at a relatively high frequency ($\simeq$1.5 T) when the upper subband starts to become occupied. This is the main feature we are associating with the annular FS.

---

[1] N. W. Ashcroft and N. D. Mermin, *Solid State Physics* (Holt, Rinehart and Winston, Philadelphia, 1976).

[2] I. M. Lifshitz, J. Exptl. Theoret. Phys. (U.S.S.R.) **38**, 1569 (1960).

[3] K. Takashina, Y. Ono, A. Fujiwara, Y. Takahashi, and Y. Hirayama, Phys. Rev. Lett. **96**, 236801 (2006).

[4] Y. P. Shkolnikov, E. P. De Poortere, E. Tutuc, and M. Shayegan, Phys. Rev. Lett. **89**, 226805 (2002).

[5] O. Gunawan, Y. P. Shkolnikov, E. P. De Poortere, E. Tutuc, and M. Shayegan, Phys. Rev. Lett. **93**, 246603 (2004).

[6] M. A. Mueed, D. Kamburov, M. Shayegan, L. N. Pfeiffer, K. W. West, K. W. Baldwin, and R. Winkler, Phys. Rev. Lett. **114**, 236404 (2015).

[7] F. T. Vasko and N. A. Prima, Fiz. Tverd. Tela **21**, 1734 (1979) [Sov. Phys. Solid State **21**, 994 (1979)].

[8] Y. A. Bychkov and E. I. Rashba, Sov. Phys. JETP Lett. **39**, 78 (1984).

[9] E. Cappelluti, C. Grimaldi, and F. Marsiglio, Phys. Rev. Lett. **98**, 167002 (2007).

[10] L. W. Cheuk, A. T. Sommer, Z. Hadzibabic, T. Yefsah, W. S. Bakr, and M. W. Zwierlein, Phys. Rev. Lett. **109**, 095302 (2012).

[11] G. Bihlmayer, O. Rader, and R. Winkler, New J. Phys. **17**, 050202 (2015).

[12] V. Brosco, L. Benfatto, E. Cappelluti, and C. Grimaldi, Phys. Rev. Lett. **116**, 166602 (2016).

[13] F. Nichele, M. Kjaergaard, H. J. Suominen, R. Skolasinski, M. Wimmer, B.-M. Nguyen, A. A. Kiselev, W. Yi, M. Sokolich, M. J. Manfra, F. Qu, A. J. A. Beukman, L. P. Kouwenhoven, and C. M. Marcus, arXiv:1605.01241.

[14] R. Winkler, *Spin-Orbit Coupling Effects in Two-Dimensional Electron and Hole Systems* (Springer, Berlin, 2003).

[15] E. McCann and V. I. Fal'ko, Phys. Rev. Lett. **96**, 086805 (2006).

[16] E. V. Castro, N. M. R. Peres, T. Stauber, and N. A. P. Silva, Phys. Rev. Lett. **100**, 186803 (2008).

[17] A. Varlet, D. Bischoff, P. Simonet, K. Watanabe, T. Taniguchi, T. Ihn, K. Ensslin, M. Mucha-Kruczynski, and V. I. Fal'ko, Phys. Rev. Lett. **113**, 116602 (2014).

[18] J. Jung, M. Polini, and A. H. MacDonald, Phys. Rev. B **91**, 155423 (2015).

[19] T. Stauber, N. M. R. Peres, F. Guinea, and A. H. Castro Neto, Phys. Rev. B **75**, 115425 (2007).

[20] S. Wu, X. Dai, H. Yu, H. Fan, and W. Yao, arXiv:1409.4733.

[21] T. Cao, Z. Li, and S. G. Louie, Phys. Rev. Lett. **114**, 236602 (2015).

[22] E. Berg, M. S. Rudner, and S. A. Kivelson, Phys. Rev. B **85**, 035116 (2012).

[23] J. Ruhman and E. Berg, Phys. Rev. B **90**, 235119 (2014).

[24] In other studies [25,26], however, the enhancement of the exchange energy at the singularity point was found to be marginal.

[25] S. Chesi and G. F. Giuliani, Phys. Rev. B **83**, 235309 (2011).

[26] T. Kernreiter, M. Governale, R. Winkler, and U. Zülicke, Phys. Rev. B **88**, 125309 (2013).

[27] See Appendixes A to D for more information.

[28] L. Onsager, Philos. Mag. **43**, 1006 (1952).

[29] Y. Liu, J. Shabani, and M. Shayegan, Phys. Rev. B **84**, 195303 (2011).

[30] Y. W. Suen, J. Jo, M. B. Santos, L. W. Engel, S. W. Hwang, and M. Shayegan, Phys. Rev. B **44**, 5947 (1991).
[31] Y. W. Suen, L. W. Engel, M. B. Santos, M. Shayegan, and D. C. Tsui, Phys. Rev. Lett. **68**, 1379 (1992).
[32] Y. Liu, A. L. Graninger, S. Hasdemir, M. Shayegan, L. N. Pfeiffer, K. W. West, K. W. Baldwin, and R. Winkler, Phys. Rev. Lett. **112**, 046804 (2014).
[33] G. Bastard, *Wave Mechanics Applied to Semiconductor Heterostructures* (Les Editions de Physique, Les Ulis Cedex, 1988).
[34] G. Dresselhaus, Phys. Rev. **100**, 580 (1955).
[35] S. J. Papadakis, E. P. De Poortere, H. C. Manoharan, M. Shayegan, and R. Winkler, Science **283**, 2056 (1999).
[36] Note that, while our samples' nominal QW width is 40 nm, in our calculations we use a width of 38 nm so that the onset of the excited subband occupation, $p = 1.2 \times 10^{11}$ cm^{-2}, matches the experimental value. There are no other adjustable parameters in the calculations.
[37] We show in Appendix C that the magneto-oscillations corresponding to this peak can be extracted via inverse FT.
[38] H. L. Stormer, A. C. Gossard, and W. Wiegmann, Solid State Commun. **41**, 707 (1982).
[39] H. L. Stormer, A. C. Gossard, and W. Wiegmann, J. Vac. Sci. Technol. **21**, 507 (1982).
[40] J. P. Lu, Ph.D. thesis, Princeton University, 1998.
[41] J. P. Lu and M. Shayegan, Phys. Rev. B **58**, 1138 (1998).
[42] M. Shayegan, J. Jo, Y. W. Suen, M. Santos, and V. J. Goldman, Phys. Rev. Lett. **65**, 2916 (1990).
[43] For example, because of the very small area of our annular FS, there could be a "magnetic blurring" of the SdH oscillations [44] or disorder-induced scattering between the inner and the outer ring [45].
[44] R. de Gail, M. O. Goerbig, and G. Montambaux, Phys. Rev. B **86**, 045407 (2012).
[45] V. V. Mkhitaryan and M. E. Raikh, Phys. Rev. B **83**, 045406 (2011).
[46] G. Liu, G. Wang, Y. Zhu, H. Zhang, G. Zhang, X. Wang, Y. Zhou, W. Zhang, H. Liu, L. Zhao, J. Meng, X. Dong, C. Chen, Z. Xu, and X. J. Zhou, Rev. Sci. Instrum. **79**, 023105 (2008).
[47] J. Shabani, T. Gokmen, Y. T. Chiu, and M. Shayegan, Phys. Rev. Lett. **103**, 256802 (2009).
[48] B. Vinter and A. W. Overhauser, Phys. Rev. Lett. **44**, 47 (1980).
[49] M. E. Raikh and T. V. Shahbazyan, Phys. Rev. B **49**, 5531 (1994).